Analytica Chimica Acta 1112 (2020) 72–79

Contents lists available at ScienceDirect

Analytica Chimica Acta

journal homepage: www.elsevier.com/locate/aca

# Point-of-care testing of MicroRNA based on personal glucose meter and dual signal amplification to evaluate drug-induced kidney injury

Xitong Huang , Jiwei Li , Mi Lu , Wangning Zhang , Zhiming Xu , Bo-Yang Yu *, Jiangwei Tian **

*State Key Laboratory of Natural Medicines, Jiangsu Key Laboratory of TCM Evaluation and Translational Research, Research Center for Traceability and Standardization of TCMs, School of Traditional Chinese Pharmacy, China Pharmaceutical University, Nanjing, 211198, PR China*

## HIGHLIGHTS

- A portable and sensitive POCT method to detect miRNA-21 based on personal glucose meters has been developed.
- A weak signal of miRNA can be significantly amplified via the DNAzyme and invertase.
- The method exhibits excellent sequence selectivity and single-base mutation can be easily discriminated.
- The dependable POCT strategy is promising to supply valuable information for evaluation of drug induce kidney injury.

## GRAPHICAL ABSTRACT

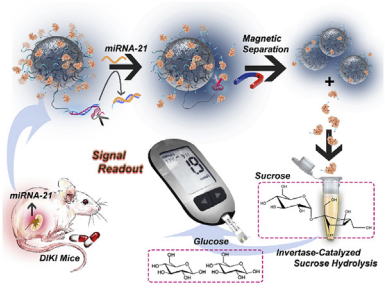


## ARTICLE INFO

*Article history:*
Received 26 November 2019
Received in revised form
24 March 2020
Accepted 25 March 2020
Available online 27 March 2020

*Keywords:*
MicroRNA
DNAzyme
Point-of-care testing
Signal amplification
Drug-induced kidney injury

## ABSTRACT

The upregulation or downregulation of microRNA-21 (miRNA-21) is closely related with drug-induced kidney injury (DIKI). As a potential and significant biomarker, the point-of-care testing (POCT) of miRNA-21 is worthy of attention and can provide essential information for clinical diagnosis. Hence, we design a portable and sensitive POCT assay for miRNA-21 using personal glucose meters (PGM). The whole operational system is constructed on streptavidin-coated magnetic beads (MBs) modified with substrate strands linked invertase and DNAzyme molecules each silenced by a locking strand. In the presence of miRNA-21, the locking strand can hybridize to miRNA-21, which originates the activation of the DNAzyme. The DNAzyme cleaves the substrate strands and induces the release of invertase from the surface of MBs. The separated invertase hydrolyzes sucrose to glucose which can be measured by PGM. The dual enzyme mediated catalyzation by DNAzyme and invertase therefore triggers the signal amplification. We establish a linear relationship between PGM and different concentration of miRNA-21 in the range of 100 fM to 1 pM. The limit of detection is 68.08 fM, which is comparable with some of the previous reports. The biosensor also exhibits excellent sequence selectivity, well-presented reproducibility and stability. Notably, by detecting miRNA-21 in urine, this method has been successfully used to predict DIKI and evaluate the protection effect of drugs on DIKI. Therefore, a dependable and low-cost POCT strategy for the detection of miRNA-21 is established, which is promising to supply valuable information for drug screening and evaluation of DIKI.



* Corresponding author.
** Corresponding author.
*E-mail addresses:* boyangyu59@163.com (B.-Y. Yu), jwtian@cpu.edu.cn (J. Tian).

https://doi.org/10.1016/j.aca.2020.03.051
0003-2670/

## 1. Introduction

MicroRNAs (miRNAs) are short endogenous noncoding small molecules with about 18–25 nucleotides and regulate the diverse gene expression by combining with messenger RNAs at post-transcriptional levels [1–4]. Growing evidence has proved that dysregulation of miRNAs are closely related to the pathophysiological processes of drug-induced kidney injury (DIKI) [5–7]. Especially, levels of miRNA-21 are reported to be significantly increased in rat kidneys with tubular injury induced, by gentamicin administration and in urine from patients with acetaminophen induced acute kidney injury [8–10]. These findings suggest that miRNA-21 may serve as potential and promising biomarker in liquid biopsy for the detection of DIKI. Therefore, accurate quantification of miRNA-21 is of great importance for the prediction and therapeutic evaluation of DIKI.

Traditional methods for miRNA analysis include Northern blotting analysis [11], quantitative reverse transcription-polymerase chain reaction (qRT-PCR) [12], oligonucleotide microarrays [13], and next-generation sequencing (NGS) [14]. However, these methods remain challenges in the sensitivity and selectivity for miRNA quantitation. Northern blotting is a long and complex procedure that requires radioactive labeling and detection limits are usually high [15]. In the process of qRT-PCR, small contaminants may also be amplified to produce false positives [16]. Oligonucleotide microarrays and NGS methods often suffer from the relatively high rate of detection errors, high demands for apparatus, and expensive cost [17,18]. In the past years, several new methods have been established for miRNA detection such as electrochemical methods [19–21], fluorescence methods [22–24], nanoparticle amplification methods [25–27], chemiluminescence methods [28–30]. Indeed, these strategies provide innovative analytical platforms for miRNA detection, but their widespread utilizations are restricted due to the requirement of complex operation and expertise, and expensive and relatively involute equipment. Therefore, it is highly meaningful and desirable to establish a sensitive, selective, facile, cost-effective, and portable method to meet the latest analytical demands for miRNA detection.

In this work, we propose a point-of-care testing (POCT) for the quantitative detection of miRNA-21 based on a personal glucose meter (PGM) and dual signal amplification. As an extensively utilized personal diagnosis equipment for POCT, PGM is available at home worldwide with low price and benefits from its portable size, simple operation and reliable quantitative results [31]. Lu's group pioneered the use of blood glucose meters for the detection of non-glucose targets in 2011 [32]. Afterwards, a series of non-glucose targets analytes such as metal ions, small molecules, and proteins based on PGM were exploited by establishing a functional relationship between target recognition and glucose generation by rational design [33–35]. However, there are still few research used PGM for miRNA detection. This motivates us to develop a miRNA detection method using PGM as the device for test readout. The relatively low sensitivity is one of the main challenge for PGM-based detection strategies. To further upgrade the detection sensitivity, a dual signal amplification strategy of invertase and RNA-cleaving DNAzyme was designed. By decorating streptavidin-coated magnetic beads (MBs) with biotinylated RNA-cleaving DNAzyme strands each silenced by a locking strand and substrate strands linked to invertase, the complex (MBs-DNA-Inv) has been developed (Scheme 1A). In the presence of miRNA-21, it hybridizes with the locking strand through a strand-displacement reaction, leading to the release of the locking strand from the DNAzyme. With the help of the cofactor $Mn^{2+}$, the DNAzyme is activated to cleave the substrate strands, which induces the release of the invertase from the surface of MBs to the solution. The autonomous operation is self-powered which is fueled by DNAzyme-catalysed substrate cleavage [36]. After magnetic separation, the supernatant involving the released invertase is transferred into sucrose solution to catalyze saccharose into glucose. The dual enzyme mediated catalyzation by DNAzyme and invertase triggers the signal amplification. Consequently, a small amount of miRNA-21 is converted to the signal of glucose concentration measured by PGM (Scheme 1B). We construct the linear relationship between miRNA-21 concentration and PGM signal. Therefore, a reliable and convenient POCT for quantitative detection of miRNA-21 has been established, which is applied to predict DIKI and evaluate the protection effect of different kinds of drugs on DIKI.

## 2. Experimental section

### 2.1. Preparation of the MBs-DNA-Inv complex

Firstly, the DNAzyme strands silenced by the locking strands were prepared before conjugation to the MBs. To ensure the complete locking of the DNAzyme strand by the locking strand, three-fold molar excess of the locking strand was used. 30 μL of 3 mM locking strand and 30 μL of 1 mM Biotin-DNAzyme strand were mixed in 0.1 M PBS buffer (pH 7.4). The mixture was then heated to 75 °C and gradually cooled to 25 °C. The MBs-DNA-Inv complex was constructed by functionalizing the MBs with the prelocked DNAzyme and its substrate. To remove the phosphate anions that adsorbed on the surface of MBs during storage, 1 mL MB (1 mg $mL^{-1}$) were soaked in Buffe A solution (pH 7.4) which contained 0.1 M NaCl, 0.1 M KCl, 0.001 M $MgCl_2$, 0.05% Tween-20, and 0.01 M 4-(2-hydroxyethyl)-1-piperazineethanesulfonic acid (HEPES) overnight on a vertical rotator, because MBs were purchased as solutions in PBS buffer and phosphate anions could compete with the binding between $Mn^{2+}$ and the DNAzyme [33]. The Biotin-DNA-Inv and Biotin-DNAzyme were prewashed by Buffer A for 5 times before being mixed with MBs. Finally, 25 μL of 1 mM Biotin-DNA-Inv and the prelocked Biotin-DNAzyme (1:1) were incubated with 1 mL MB (1 mg $mL^{-1}$) for 2 h while rolling, then MBs-DNA-Inv complex was washed 3 times by magnetic separation, dispersed in 1 mL of Buffer C (0.2 M NaCl, 0.05 M 2-(*N*-morpholino) ethanesulfonic acid (MES) buffer, pH 5.5, 0.05% Tween-20) and stored at 4 °C.

### 2.2. Detection of miRNA-21 with MBs-DNA-Inv and PGM

60 μL MB–DNA-Inv solution was put in a magnetic frame for 3 min, and the supernatant was abandoned. Then, 60 μL Buffer B (pH 8.0) containing 25 mM Tris-acetate and 200 mM NaCl, 10 μL of varying concentrations of miRNA-21 and 10 μL $MnCl_2$ were added and incubated at room temperature for 40 min. The reaction was stopped by 50 mM Ethylenediaminetetraacetic acid (EDTA). Afterwards, the mixture was put close to the magnetic frame. The supernatant was dropped into a tube with 100 μL of 1 M sucrose. The mixture was heated to 55 °C for 40 min and then performed PGM measurement.

### 2.3. Animal model and experiments

Male Institute for Cancer Research (ICR) mice were purchased from the Laboratory Animal Center and Institute of Comparative Medicine at Yangzhou University. All animal study protocols were designed in according to guidelines set by the National Institute of Health Guide for the Care and Use of Laboratory Animals and approved by the Animal Ethical Experimentation Committee of China Pharmaceutical University. Mice weighing 20–25 g were housed with

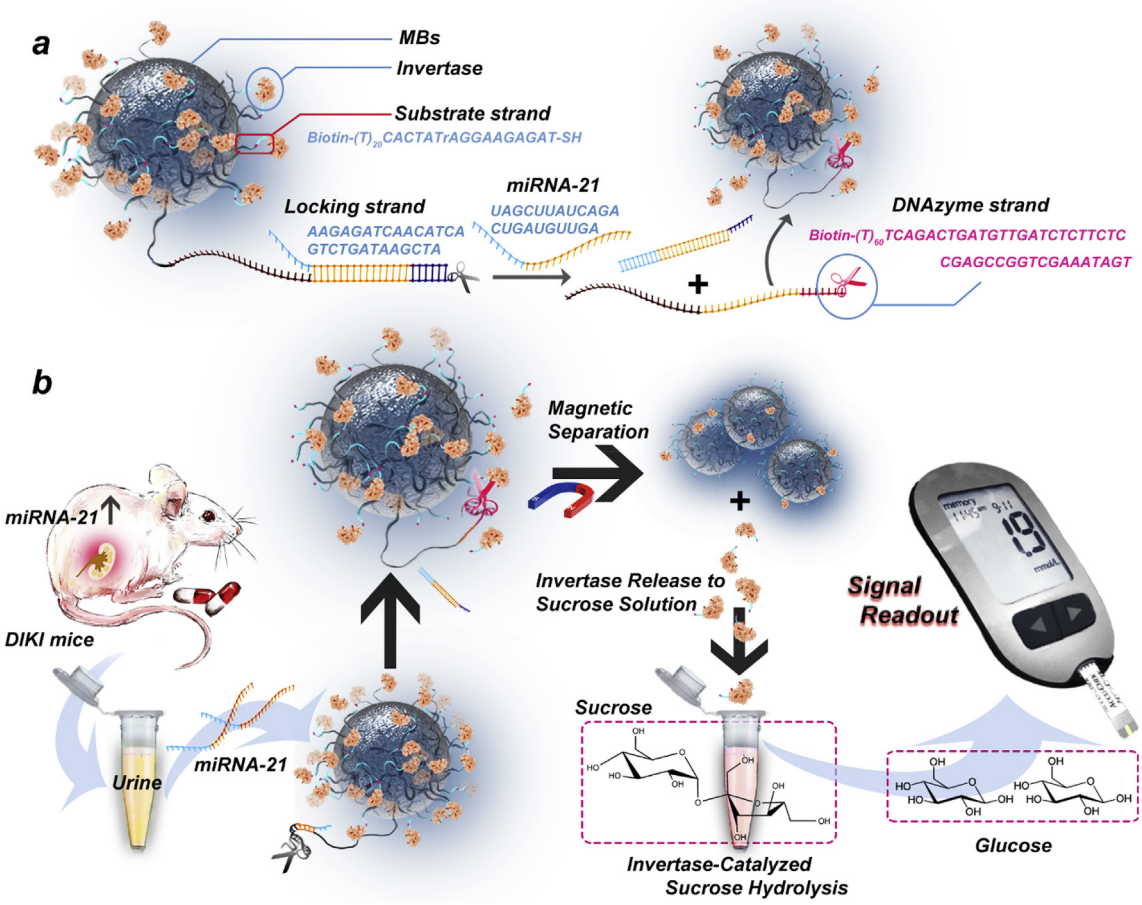


**Scheme 1.** Schematic Diagram of (A) Constitution of MBs-DNA-Inv and (B) Mechanism for the detection of miRNA-21 based on PGM and Dual Signal Amplification to Evaluate DIKI.

12:12 h light: dark cycle and were allowed free access to food and water. Mice were divided into twelve groups (6 mice per group). Mice of groups from one to four were given a single intraperitoneal injection of cis-diammine platinum dichloride (CDDP, 20 mg $kg^{-1}$). Mice of groups from five to eight were given a single intraperitoneal injection of aristolochic acids (AA, 50 mg $kg^{-1}$). Mice of groups from nine to twelve served as control groups received a same volume of normal saline solution. Groups of mice were separately killed at 0, 24, 48, 72 h after intraperitoneal injection. The body weight of each mouse was recorded before drug administration and the following days until euthanasia. Urine samples were collected via metabolic cage. Blood samples were collected from orbital vein of mice and centrifuged at 3000 rpm for 15 min at 4 °C to separate serum. The urine and serum samples were stored at −80 °C for the determination of biochemical indicators. Renal function was assessed by measuring Serum creatinine (sCrea), blood urea nitrogen (BUN) and miRNA-21 relative expression levels in urine. The levels of sCrea, BUN in serum were measured through relevant assay kits. The total RNA was extracted from mice urine by the expression of the miRNA extraction kit and the extracted miRNA was separately detected by our proposed method and qRT-PCR. Part of the kidney samples were performed for hematoxylin eosin (HE) staining in order to observe pathological changes in renal tissue, degrees of fibrosis tissue hyperplasia, structures of glomeruli and tubules, arrangement of tubules and urate deposition.

### *2.4. The protective effect of drugs on CDDP/AA induced renal injury*

Mice were randomly divided into control group, CDDP group, AA group, CDDP + *N*-acetylcysteine (NAC) group, CDDP + HuangKui capsule (HK) group, AA + NAC group, AA + HK group. Each group contained 6 mice. Control group comprised healthy control mice treated with normal saline; CDDP group comprised DIKI mice received one single dose of 20 mg $kg^{-1}$ CDDP via intraperitoneal; AA group comprised DIKI mice received one single dose of 50 mg $kg^{-1}$ AA via intraperitoneal; CDDP + NAC group comprised mice were administered orally with NAC (0.1 g $kg^{-1}$) once daily for 14 consecutive days before treated with CDDP; CDDP + HK comprised mice were administered orally with HK (1.25 g $kg^{-1}$) once daily for 14 consecutive days before treated with CDDP; AA + NAC group comprised mice were administered orally with NAC (0.1 g $kg^{-1}$) once daily for 14 consecutive days before treated with AA; AA + HK comprised mice were administered orally with HK (1.25 g $kg^{-1}$) once daily for 14 consecutive days before treated with AA. After 14 days' administration cycle, mice with water but no food for twelve hours were killed. The body weight of each mouse was recorded before drug administration and the following days until euthanasia. The blood samples were collected for the determination of biochemical indicators. The urine samples were collected for miRNA assay.

## 3. Results and discussion

### 3.1. Analysis of free DNAzyme performance in solution

Gel electrophoresis was used to analysis the strand displacement efficiency of locking strand between target and DNAzyme strand (Fig. 1). For easier operation, a DNA strand with the same sequence was used as miRNA-21 replacement in the experiment. As shown in lane 6, DNAzyme was inactive without target DNA because the DNAzyme was isolated by the locking strand, with an evidence of unobservable increase product band on PAGE. In the presence of target DNA, a strong band about 25 bp in lane 7 was observed, indicating the hybridization of locking strand with the target DNA. At the same time, the absence of target DNA in lane 7 supported the complete displacement reaction of the prelocked DNAzyme strand by the target DNA. When the strand displacement was triggered, the DNAzyme was exposed to a substrate strand and allowed to the cleavage reaction. Divalent metal cofactors are often demanded to obtain the catalytic activity of DNAzymes. It is reported that the best auxiliary ion in the truncated form of DNAzyme17-8 E is $Mn^{2+}$ ion [22]. When cofactor $Mn^{2+}$ was added into the mixture, DNAzyme was activated to cleave the substrate strand, causing the releasing of invertase from the MBs. A continuous increase in product fragment (F1) over 60 min operating period indicated successful cutting of the DNAzyme (Fig. S1A). In the absence of $Mn^{2+}$, no fragment product was observed (Fig. S1B), verifying that the manipulation of DNAzyme movement relied on specific sequences and $Mn^{2+}$.

### 3.2. Characterization of DNA-Inv conjugate and MBs-DNA-Inv complex

Maleimide-thiol reaction by the heterobifunctional linker (sulfosuccinimidyl-4-(*N*-maleimidomethyl) cyclohexane-1-carboxylate, sulfo-SMCC) was utilized to synthesize the DNA-Inv conjugate [33,34]. The purified DNA-Inv conjugate was characterized by UV–Vis absorption spectra and PAGE images. As shown in Fig. S2, the purified DNA-Inv conjugate displayed an UV–vis absorption spectrum which covered well with the sum of the spectra of individual DNA and invertase. The successful conjugation had also been verified by SDS-PAGE, while the migration of invertase was more than that of the DNA-Inv conjugate band (Fig. S3). Because of each DNA is around 7 K and there should be more than 20 amine groups in each invertase for conjugation with substrate strand, the conjugation increased the molecular weight of the invertase. The dynamic light scattering (DLS) spectrum suggested the MBs solution an average hydration diameter of 1.13 ± 0.058 μM with a uniform distribution. After modifying the DNA-Inv conjugate, hydration diameter increased to about 1.73 ± 0.12 μM (Fig. S4A), indicating the successful synthesis of MBs-DNA-Inv. In addition, the zeta-potentials of MBs and MBs-DNA-Inv were significantly different. The pure MBs had the zeta potential of −8.54 ± 0.23 mV. After conjunction, the zeta potential of MBs-DNA-Inv was decreased to be −19.62 ± 0.38 mV (Fig. S4B), which indicated that the MBs-DNA-Inv was highly dispersible in aqueous solution [37].

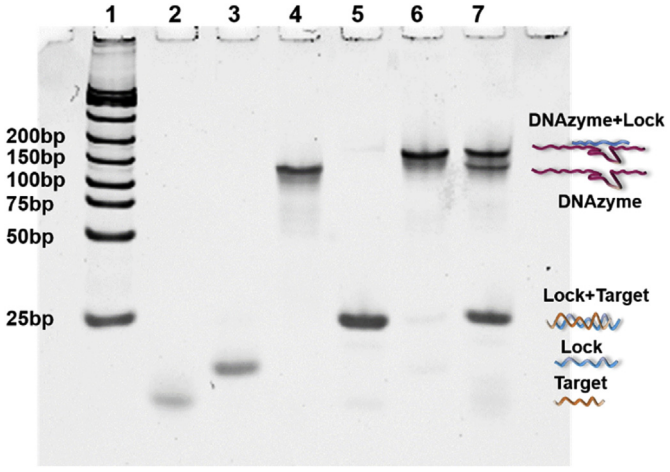


**Fig. 1.** 12% PAGE gel image assay for stand displacement of DNAzyme by target DNA. Lane 1: DNA ladder; lane 2: target DNA; lane 3: locking strand; lane 4: DNAzyme strand; lane 5: mixture of locking strand and target DNA at 1:1 molar ratio; lane 6: mixture of locking strand and DNAzyme strand at 1:1 molar ratio; lane 7: mixture of locking strand-DNAzyme strand complex and target DNA at 1.1:1 molar ratio.

### 3.3. Optimization of experimental conditions

For the purpose of acquiring the high performance of detection platform, the reaction conditions including temperature, buffer pH, incubation time and the dosage of $Mn^{2+}$ were investigated. Incubation temperature was a critical factor because it could influence the enzyme activity, hybridization efficiency and stability of DNA/RNA hybrids. A series of reaction temperature (0 °C, 4 °C, 25 °C, 37 °C, 45 °C) were studied. The PGM value reached maximum at 25 °C (Fig. 2A) which was selected for subsequent detection. This could be attributed that a higher or lower hybridization temperature could induce an ineffective or nonspecific hybridization. We also studied the performance of MBs-DNA-Inv under different pH conditions. The system exhibited dependable performance at pH values of 8.0–8.5 (Fig. 2B) due to the best cutting efficiency of DNAzyme in this pH range. A buffer of pH 8.0 was used in the subsequent experiments. Moreover, the incubation time for miRNA-21 detection was also evaluated. In the presence of 400, 800 or 1000 fM miRNA-21, the glucose concentration increased gradually with time (Fig. 2C). Since an excess of sucrose (1 M) was added to obtain the maximum reaction rate, the kinetics of glucose production should depend on the concentration of miRNA-21 in the sample. The more target miRNA-21 in solution, the earlier the sample will display a detectable signal. To obtain a better signal-to-background level, 40 min was selected as the incubation time. $Mn^{2+}$ ion was necessary for the catalytic activity of DNAzyme [22]. When $Mn^{2+}$ ion was added to the mixture, the DNAzyme cleaved the substrate strand at the single-ribonucleotide junction which brought about two nucleic acid segments and released the invertase to the solution. To explore the optimal concentration of $Mn^{2+}$ in solution, we added different concentrations of $Mn^{2+}$ in the solution in the presence of 1000 fM miRNA-21. The results revealed the PGM value reached a plateau stage when the concentration of $Mn^{2+}$ was 8 mM (Fig. 2D). In order to ensure sufficient ion initiation in practical applications, 10 mM $Mn^{2+}$ was selected as the starter ion in the reaction system.

### 3.4. Sensitivity, specificity, reproducibility and stability for miRNA-21 detection using MBs-DNA-Inv and PGM

The sensitivity for miRNA-21 detection using MBs-DNA-Inv and PGM was carried out under optimized conditions. The PGM signal increased with increasing concentrations of miRNA-21 (Fig. 3A). A good linear range from 100 to 1000 fM was obtained (Fig. 3A, Inset) with the linear regression equations $S = 2.55 + 0.029\ c$, in which S was the value of PGM reading and c was the miRNA-21 concentration. The coefficient of determination ($R^2$) was 0.995. The limit of detection ($3\sigma/k$, in which was the standard deviation of blank measurements, $n = 6$, and k was the slope of the linear equation)

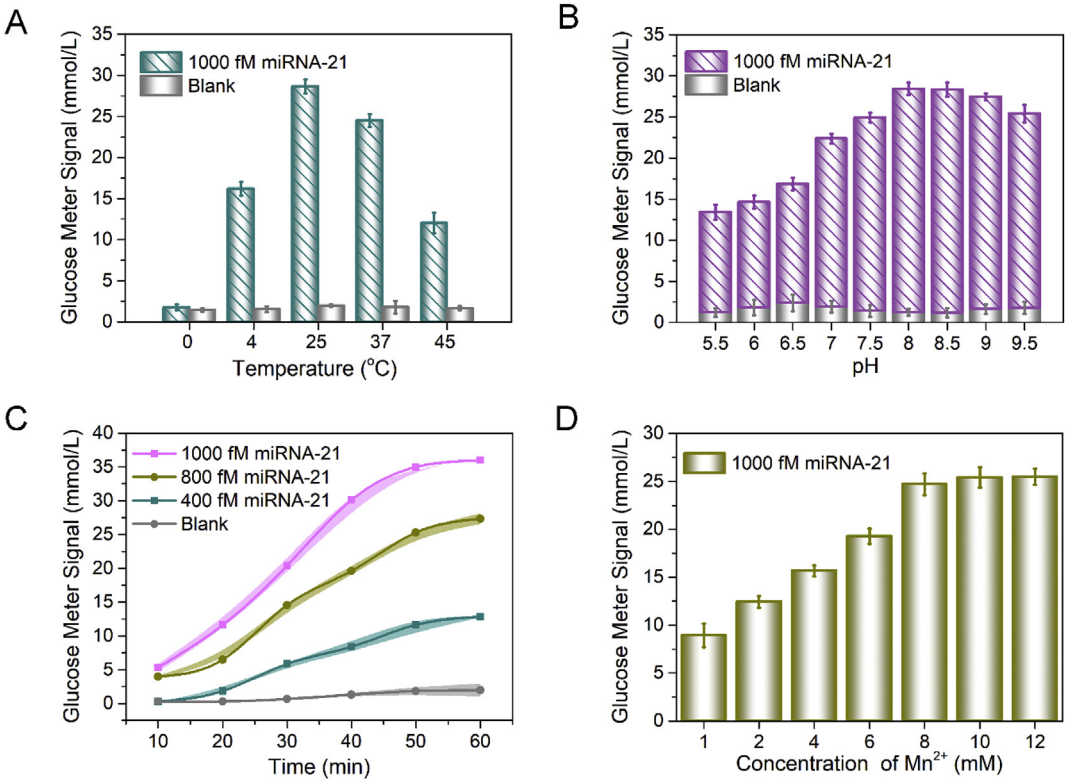


**Fig. 2.** Optimization based on MBs-DNA-Inv for miRNA-21 assay. Effects of the reaction (A) temperature, (B) pH, (C) time, and (D) concentration of Mn2+ for target miRNA-21 detection. Data are means ± SD (n = 3).

for miRNA-21 was determined to be 68.08 fM, which is comparable or even better than some of other reported researches [35,38,39].

Specificity was also the crucial factor to evaluate the effectiveness and practicability of the proposed POCT strategy. The perfectly-matched miRNA-21, single-base mismatched miRNA-21 (Mis-1, Mis-2, Mis-3), and non-complementary miRNA-4640, miRNA-423, miRNA-200c were used to evaluate the specificity of our method (detail sequences were shown in Table S1). As shown in Fig. 3B, significant PGM signal was only detected in the presence of perfectly-matched miRNA-21, the signals of other miRNA were close to the blank signal, indicating that the interference was almost negligible. The MBs-DNA-Inv platform could efficaciously distinguish the fully matched target from variants of single-base mismatch. Therefore, the proposed POCT strategy possessed high specificity for miRNA assay.

The reproducibility and stability are important features for the practical application of biosensor. The reproducibility of the MBs-DNA-Inv complex was investigated by testing different concentration of miRNA-21 samples (200 fM, 500 fM, 1000 fM). As shown in Table S2, the relative standard deviation (RSD) for the parallel detection of 200, 500, and 1000 fM miRNA-21 with 10 batches of MBs-DNA-Inv, respectively, were 3.9%, 3.0%, and 3.6%. The results exhibited high reproducibility of this assay. Then, the stability of the MBs-DNA-Inv complex for miRNA-21 detection was also studied. MBs-DNA-Inv was stored at 4 °C (in a refrigerator) and used to measure the same concentration miRNA-21 at intervals of 7 days. As seen from Fig. S5**,** no obvious change of PGM signals were observed after 4 weeks and the RSD was calculated to be <3.6%, indicating that the detection platform was highly stable. These results demonstrated that MBs-DNA-Inv complex were reliable on the basis of the excellent reproducibility and in storage conditions and it provided the possibility for routine analysis.

### 3.5. Detection of miRNA-21 in urine sample

MiRNA-21 expression profiles in urine were reported related to classification, diagnosis and disease progression of DIKI [40,41]. Herein, different amounts of miRNA-21 were mixed with the urine samples and obtained a serious of final concentrations (100 fM, 200 fM, 400 fM600 fM, 800 fM, 1000 fM). A positive linear response between the miRNA-21 concentration (100–1000 fM) and PGM signals for the detection in urine ($S = 2.35 + 0.029\ c$; $R^2 = 0.991$, in which S is the value of PGM readings and c is the miRNA-21 concentration) was obtained and shown in Fig. S6, which indicated that this method was also suitable for miRNA-21 detection under urine environment. To further confirm the accuracy of this method, the detection of miRNA-21 in real diluted mice urine sample was researched using standard addition according the previous reports [42]. We spiked different concentrations of miRNA-21 (200 fM, 500 fM, 800 fM, 1000 fM) into the urine samples and got the recovery rate. As shown in Table 1, the recovery rate varied from 95.8% to 106.8%, implying that the matrix effects of this method was negligible and providing the strategy to be a possible vista for the detection of miRNAs in real biological urine samples.

### 3.6. MiRNA-21 detection in urine samples of DIKI mice

To further confirm the practicality of this strategy, we tested miRNA-21 expression level in urine samples from renal injury mice caused by CDDP. CDDP is one of the most used chemotherapeutic agents for cancer treatment while its nephrotoxicity is also obviously [43,44]. The mice in CDDP group were shown varying degrees of poisoning symptoms after receiving CDDP treatment, including lethargy, depression, inappetence, dullness, weakness, change in behavior, disinclination to move, and loss of hair. Besides, the body

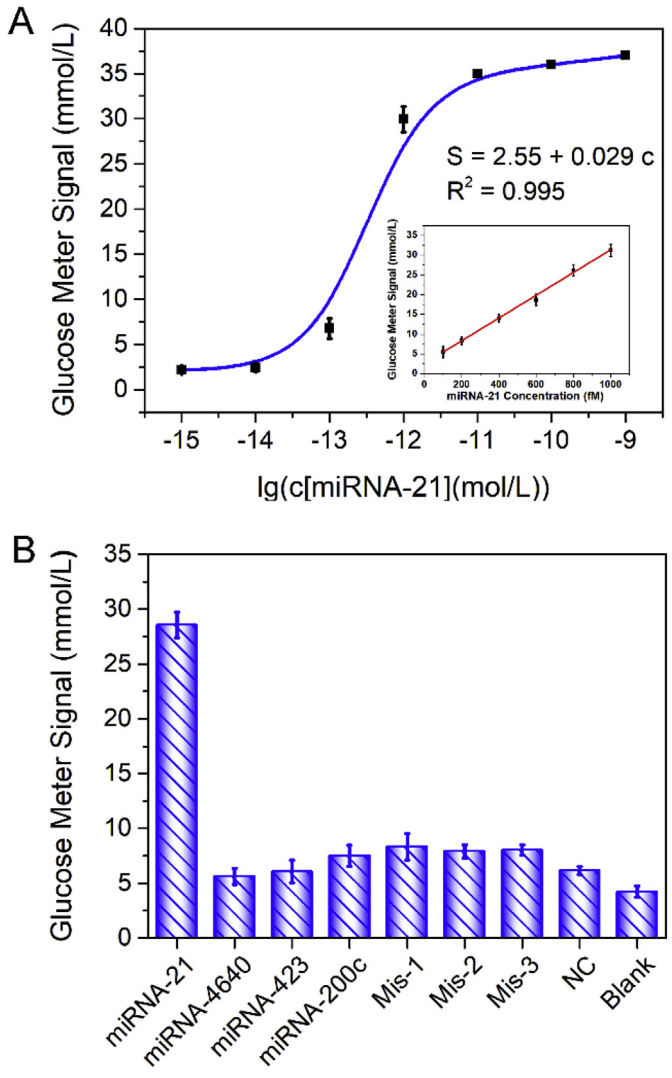


**Fig. 3.** Sensitivity and selectivity of the POCT assay for miRNA-21 detection. (A) Relationship between the concentration of miRNA-21 and PGM signal. Inset: a linear standard curve from 100 to 1000 fM. (B) Response of PGM for the detection of different miRNAs by the POCT assay. The concentration of miRNAs was 1000 fM. Data are means ± SD (n = 3).

**Table 1**
Recovery Test for Assay of Target miRNA-21 in Urine of Mice.

| Added (fM) | Detected (fM) | Recovery (%) | RSD% (n = 3) |
|---|---|---|---|
| 200.0 | 193.7 | 96.8 | 3.7 |
| 500.0 | 533.9 | 106.8 | 2.6 |
| 800.0 | 838.5 | 104.8 | 2.9 |
| 1000.0 | 958.0 | 95.8 | 2.6 |

weight of the mice in CDDP group reduced obviously compared to control group (Fig. S7A). We tested miRNA-21 expression level in urine samples by our method and compared the results with current benchmark for miRNA detection in the laboratory, that is, qRT-PCR. 10 μg of total miRNA was extracted from each urine sample. Then by using MBs-DNA-Inv and qRT-PCR (Fig. S8), we acquired the relative expression level of miRNA-21 under optimal conditions. As demonstrated in Fig. 4A, the relative miRNA-21 expression level obtained by our method was in consonance with those by qRT-PCR, which were increased significantly compared to the control group at the same time point. In the meantime, in order to evaluate the level of CDDP-induced kidney injury carefully, the conventional clinical examination biomarkers (sCrea and BUN) were detected. The concentration of sCrea (Fig. S9A) and BUN (Fig. S9B) increased obviously after CDDP treatment, suggesting a serious damage of renal injury. The kidneys of mice were received to carry out histopathological examination by hematoxylin-eosin (HE) staining, further supporting evidence of CDDP induced kidney injury (Fig. S10). These results clearly demonstrated the potential of our proposed assay for application in real bioanalysis of DIKI.

Furthermore, MBs-DNA-Inv and PGM based method was expanded to monitor the AA induced kidney injury. AA was another compound that could induce acute kidney injury [45]. The relative expression level of miRNA-21 in urine samples tested by our method increased about 2 fold after 72 h AA treatment, which was consistent with the result of qRT-PCR (Fig. 4B). Similar to previous experiments, the substance of sCrea (Fig. S11A) and BUN (Fig. S11B) increased obviously after AA treatment. The reduced body weight (Fig. S7B) and HE staining results (Fig. S10) confirmed a severe damage in kidney. Taken together, these results suggested that our method was suitable and general for the prediction of DIKI.

### 3.7. Evaluation of protective effect of drug on DIKI

The MBs-DNA-Inv and PGM system was used to evaluate the protective effect of drug on CDDP or AA induced renal injury. NAC is an antioxidant with nephroprotective effect in animal models of different forms of DIKI [46,47]. The efficacy of NAC in preclinical models is thought to be based on its capacity to inhibit oxidative stress, a key pathophysiological element in DIKI. Additionally, HK capsule was chosen as representative Chinese patent medicine for protecting the renal injury [48]. The pretreatment with NAC or HK in the mice treated with CDDP could remarkably inhibited the relative expression of miRNA-21 (Fig. 4C), the elevation of sScrea (Fig. S12A) and BUN (Fig. S12B), suggesting the dramatically protective effect of these two kinds of drugs on CDDP induced kidney injury. This conclusion was also supported by body weight change (Fig. S13) and HE staining (Fig. S14). However, the effect of NAC on DIKI caused by AA was not significant (Fig. 4D), probably because AA was genotoxic to the renal cells [49]. Notably, the relative expression of miRNA-21 decreased significantly for the AA + HK group compared with the AA group (Fig. 4D), indicating good protective effect of HK on AA-induced kidney damage. The result implied that HK may have better comprehensive protective effects on this kind of drug induced kidney injury. All in all, these results demonstrated that our platform could be employed to evaluate the protective effect of drugs on DIKI which was promising for protective drug screening.

## 4. Conclusions

In brief, we have designed a POCT method for the detection of miRNA-21 based on MBs-DNA-Inv and PGM. A small amount of miRNA-21 can be converted to amplified glucose signal via DNAzyme and invertase. This method provides a low detection limit of 68.08 fM for miRNA-21 detection. The target-dependent locking strand effectively improves the specificity and the single-base mutation can be easily discriminated. The biosensor also exhibits well-presented reproducibility and stability. It should be noted that our method has been successfully used for the prediction of DIKI by detecting the relative expression level of miRNA-21 in urine sample collected from DIKI mice and the results are in consistence with the result of qRT-PCR. Furthermore, evaluation of the protection effect of drugs on DIKI using this method has been demonstrated to be practicable by detecting miRNA-21. Therefore, a convenient and

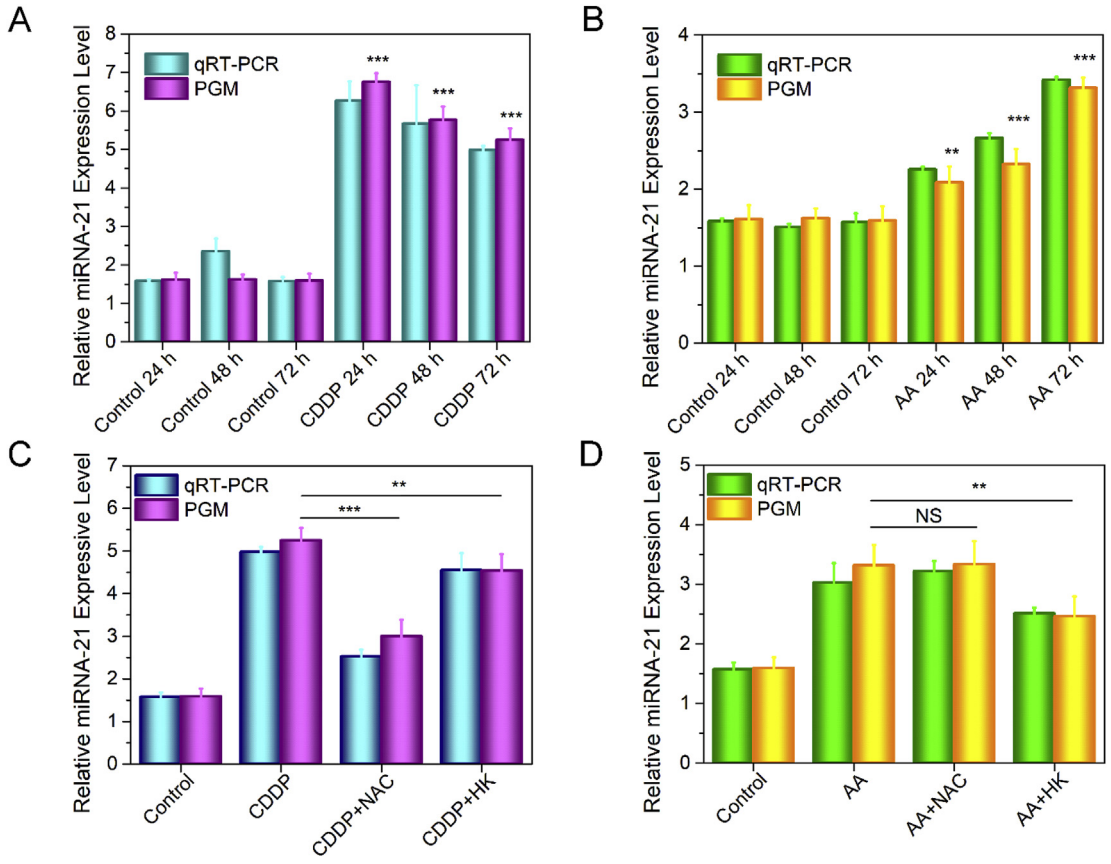


**Fig. 4.** qRT-PCR and PGM based method for quantification of the relative miRNA-21 expression level from urine samples of the mice treated with (A) CDDP or (B) AA to induce kidney injury. Data represent means ± SD (n = 6), *$P < 0.05$, **$P < 0.01$, ***$P < 0.001$, compared with control group at the same time point using a Student's *t*-test. qRT-PCR and PGM based method for quantification of the relative miRNA-21 expressive level from urine samples of the mice pretreated with NAC or HK and then treated with (C) CDDP or (D) AA. Data represent means ± SD (n = 6), *$P < 0.05$, **$P < 0.01$, ***$P < 0.001$, NS (non-significant) for comparison using a Student's *t*-test.

practicable POCT strategy for the detection of miRNA-21 is established, which is promising to supply valuable information for DIKI evaluation and protective drugs screening.

## Declaration of competing interest

The authors declare that they have no known competing financial interests or personal relationships that could have appeared to influence the work reported in this paper.

## CRediT authorship contribution statement

**Xitong Huang:** Conceptualization, Investigation, Writing - original draft. **Jiwei Li:** Conceptualization, Data curation. **Mi Lu:** Visualization, Methodology. **Wangning Zhang:** Formal analysis. **Zhiming Xu:** Validation. **Bo-Yang Yu:** Supervision. **Jiangwei Tian:** Project administration, Funding acquisition, Writing - review & editing.

## Acknowledgements

This research was supported by National Natural Science Foundation of China (21775166), Natural Science Foundation for Distinguished Young Scholars of Jiangsu Province (BK20180026), and "Double First-Class" University Project (CPU2018GF06, CPU2018GY32).

## Appendix A. Supplementary data

Supplementary data to this article can be found online at https://doi.org/10.1016/j.aca.2020.03.051.

## References

[1] V. Ambros, The functions of animal microRNAs, Nature 431 (2004) 350–355.
[2] D.P. Bartel, MicroRNAs: genomics, biogenesis, mechanism, and function, Cell 116 (2004) 281–297.
[3] H.D. Yuan, D. Mischoulon, M. Fava, M.W. Otto, Circulating microRNAs as biomarkers for depression: many candidates, few finalists, J. Affect. Disord. 233 (2018) 68–78.
[4] I. Negoi, S. Hostiuc, M. Sartelli, R.I. Negoi, M. Beuran, MicroRNA-21 as a prognostic biomarker in patients with pancreatic cancer a systematic review and metal-analysis, Am. J. Surg. 124 (2017) 515–524.
[5] A. Zarjou, S. Yang, E. Abraham, A. Agarwal, G. Liu, Identification of a microRNA signature in renal fibrosis: role of miR-21, Am. J. Physiol. Ren. Physiol. 301 (2011) F793–F801.
[6] J.M. Lorenzen, H. Haller, T. Thum, MicroRNAs as mediators and therapeutic targets in chronic kidney disease, Nat. Rev. Nephrol. 7 (2017) 286–294.
[7] Y.F. Li, Y. Jing, J.L. Hao, N.C. Frankfort, X.S. Zhou, B. Shen, X.Y. Liu, L.H. Wang, R.S. Li, MicroRNA-21 in the pathogenesis of acute kidney injury, Protein, Cell 4 (2013) 813–819.
[8] Z.H. Li, X. Deng, Z.J. Kang, Y. Wang, T.H. Xia, N. Ding, Y. Yin, Elevation of miR-21, through targeting MKK3, may be involved in ischemia pretreatment protection from ischemia–reperfusion induced kidney injury, J. Nephrol. 29 (2016) 27–36.
[9] E. Tsitsiou, M.A. Lindsay, MicroRNAs and the immune response, Curr. Opin. Pharmacol. 29 (2009) 343–351.
[10] M. Pavkovic, C. Robinson-Cohen, A.S. Chua, O. Nicoara, M. Cárdenas-González, V. Bijol, K. Ramachandran, L. Hampson, M. Pirmohamed, D.J. Antoine, G. Frendl, J. Himmelfarb, S.S. Waikar, S. Vaidya, Detection of drug-induced acute kidney injury in humans using urinary kim-1, miR-21, -200c and -423, Toxicol. Sci. 152 (2016) 205–213.

[11] E. Koscianska, J. Staregaroslan, L.J. Sznajder, M. Olejniczak, P. Galkamarciniak, W.J. Krzyzosiak, Northern blotting analysis of microRNAs, their precursors and RNA interference triggers, BMC Mol. Biol. 2 (2011) 14.
[12] S. Honda, Y. Kirino, Dumbbell-PCR: a method to quantify specific small RNA variants with a single nucleotide resolution at terminal sequences, Nucleic Acids Res. 43 (2015) e77.
[13] N. Rosenfeld, R. Aharonov, E. Meiri, S. Rosenwald, Y. Spector, M. Zepeniuk, H. Benjamin, N. Shabes, S. Tabak, A. Levy, D. Lebanony, Y. Goren, E. Silberschein, N. Targan, A. Benari, S. Gilad, N. Sionvardy, A. Tobar, M. Feinmesser, O. Kharenko, MicroRNAs accurately identify cancer tissue origin, Nat. Biotechnol. 26 (2008) 462–469.
[14] A.M. Kietrys, W.A.A. Velema, E.T. Kool, Fingerprints of modified RNA bases from deep sequencing profiles, J. Am. Chem. Soc. 139 (2017) 17074–17081.
[15] E. Várallyay, J. Burgyán, Z. Havelda, MicroRNA detection by northern blotting using locked nucleic acid probes, Nat. Protoc. 3 (2008) 190–196.
[16] H.H. Wang, H. Wang, X. Duan, Y. Sun, X. Wang, Z. Li, Highly sensitive and multiplexed quantification of mRNA splice variants by the direct ligation of DNA probes at the exon junction and universal PCR amplification, Chem. Sci. 8 (2017) 3635–3640.
[17] J.G. Hacia, Resequencing and mutational analysis using oligonucleotide microarrays, Nat. Genet. 21 (1999) 42–47.
[18] L. Liu, Y.H. Li, S.L. Li, N. Hu, Y.M. He, R. Pong, D.N. Lin, L.H. Lu, M. Law, Comparison of next-generation sequencing systems, J. Biomed. Biotechnol. 7 (2012) 1–11.
[19] K.M. Koo, L.G. Carrascosa, M.J.A. Shiddiky, M. Trau, Poly(A) Extensions of miRNAs for amplification-free electrochemical detection on screen-printed gold electrodes, Anal. Chem. 88 (2016) 2000–2005.
[20] C.S. Fang, K.S. Kim, B. Yu, S. Jon, M.S. Kim, H. Yang, Ultrasensitive electrochemical detection of miRNA-21 using a zinc finger protein specific to DNA–RNA hybrids, Anal. Chem. 89 (2017) 2024–2031.
[21] L. Tian, K. Qian, J. Qi, Q. Liu, C. Yao, W. Song, Y. Wang, Gold nanoparticles superlattices assembly for electrochemical biosensor detection of microRNA-21, Biosens. Bioelectron, 99 (2018) 564–570.
[22] H. Peng, X.F. Li, H. Zhang, X.C. Li, A microRNA-initiated DNAzyme motor operating in living cells, Nat. Commun. 8 (2017) 14378.
[23] L. Wang, R. Deng, J. Li, Target-fueled DNA walker for highly selective miRNA detection, Chem. Sci. 12 (2015) 6777–6782.
[24] P.X. Li, M. Wei, F. Zhang, J. Su, W. Wei, Y.J. Zhang, S.Q. Liu, A novel fluorescence switch for microRNA imaging in living cells based on DNAzyme amplification strategy, ACS Appl. Mater. Interfaces 10 (2018) 43405–43410.
[25] J. Su, D.F. Wang, L. Nörbel, J.L. Shen, Z.H. Zhao, Y.Z. Dou, T.H. Peng, J.Y. Shi, S. Mathur, C.H. Fan, S.P. Song, Multicolor gold-silver nano-mushrooms as ready-to-use SERS probes for ultrasensitive and multiplex DNA/miRNA detection, Anal. Chem. 89 (2017) 2531–2538.
[26] H.L. Shuai, K.J. Huang, W.J. Zhang, X. Cao, M.P. Jia, Sandwich-type microRNA biosensor based on magnesium oxide nanoflower and graphene oxide–gold nanoparticles hybrids coupling with enzyme signal amplification, Sensor. Actuator. B Chem. 243 (2017) 403–411.
[27] D. Zhu, W. Liu, D.X. Zhao, Q. Hao, J. Li, J.X. Huang, J.Y. Shi, J. Chao, S. Su, L.H. Wang, Label-free electrochemical sensing platform for microRNA-21 detection using thionine and gold nanoparticles co-functionalized $MoS_2$ nanosheet, ACS Appl. Mater. Interfaces 9 (2017) 35597–35603.
[28] Q. Wang, B.C. Yin, B.C. Ye, A novel polydopamine-based chemiluminescence resonance energy transfer method for microRNA detection coupling duplex-specific nuclease-aided target recycling strategy, Biosens. Bioelectron. 80 (2016) 366–372.
[29] Q.M. Feng, Y.Z. Shen, M.X. Li, Z.L. Zhang, W. Zhao, J.J. Xu, H.Y. Chen, Dual-wavelength electrochemiluminescence ratiometry based on resonance energy transfer between Au nanoparticles functionalized g-C3N4 nanosheet and $Ru(bpy)32^{+}$ for microRNA detection, Anal. Chem. 88 (2017) 937–944.
[30] D. Chen, S. Wen, R. Peng, Q. Gong, J. Fei, Z. Fu, C. Weng, M. Liu, A triple signal amplification method for chemiluminescent detection of the cancer marker microRNA-21, Mikrochim. Acta 186 (2019) 410.
[31] A. Heller, B. Feldman, Electrochemical glucose sensors and their applications in diabetes management, Chem. Rev. 108 (2008) 2482–2505.
[32] Y. Xiang, Y. Lu, Using personal glucose meters and functional DNA sensors to quantify a variety of analytical targets, Nat. Chem. 3 (2011) 697–703.
[33] Y. Xiang, Y. Lu, Portable and quantitative detection of protein biomarkers and small molecular toxins using antibodies and ubiquitous personal glucose meters, Anal. Chem. 84 (2012) 4174–4178.
[34] L. Yan, Z. Zhu, Y. Zou, Y.S. Huang, D.W. Liu, S.S. Jia, D.M. Xu, M. Wu, Y. Zhou, S. Zhou, Target-responsive "sweet" hydrogel with glucometer readout for portable and quantitative detection of non-glucose targets, J. Am. Chem. Soc. 135 (2013) 3748–3751.
[35] Y. Jia, F. Sun, N. Na, J. Ouyang, Detection of p53 DNA using commercially available personal glucose meters based on rolling circle amplification coupled with nicking enzyme signal amplification, Anal. Chim. Acta 1060 (2019) 64–70.
[36] D. Morrison, M. Rothenbroker, Y.F. Li, DNAzymes: selected for applications, small, Methods 3 (2018) 1700319.
[37] R.L. Xu, Progress in nanoparticles characterization: sizing and zeta potential measurement, Particuology 2 (2008) 112–115.
[38] M.H. Shamsi, K. Choi, A.H.C. Ngabc, M.D. Chamberlain, A.R. Wheeler, Electrochemiluminescence on digital microfluidics for microRNA analysis, Biosens. Bioelectron. 77 (2016) 845–852.
[39] C. Feng, X. Mao, H. Shi, B. Bo, X. Chen, T. Chen, X. Zhu, G. Li, Detection of microRNA: a point-of-care testing method based on a pH-responsive and highly efficient isothermal amplification, Anal. Chem. 89 (2017) 6631–6636.
[40] R. Nassirpour, S.K. Ramaiah, L.O. Whiteley, Nephron segment specific microRNA biomarkers of pre-clinical drug induced renal toxicity: opportunities and challenges, Toxicol. Appl. Pharmacol. 312 (2016) 34–41.
[41] S. Bhayana, F. Song, J. Jacob, P. Fadda, N.C. Denko, M. Xu-Welliver, A. Chakravarti, N.K. Jacob, Urinary mirnas as biomarkers for noninvasive evaluation of radiation-induced renal tubular injury, Radiat. Res. 188 (2017) 626–635.
[42] J. Lei, L. Shi, B. Li, C.J. Yang, Y. Jin, Ultrasensitive and portable assay of mercury (II) ions via gas pressure as readout, Biosens. Bioelectron. 122 (2018) 32–36.
[43] L. Jiang, Y. Liu, P. He, J. Chen, S. Liu, N. Tan, Geraniin ameliorates cisplatin-induced nephrotoxicity in mice, Free Radic. Res. 50 (2016) 813–819.
[44] E. Mahgoub, S.M. Kumaraswamy, K.H. Kader, B. Venkataraman, S. Ojha, E. Adeghate, M. Rajesh, Genipin attenuates cisplatin-induced nephrotoxicity by counteracting oxidative stress, inflammation, and apoptosis, Biomed. Pharmacother. 93 (2017) 1083–1097.
[45] L. Yang, T. Su, X.M. Li, X. Wang, S.Q. Cai, L.Q. Meng, W.Z. Zou, H.Y. Wang, Aristolochic acid nephropathy: variation in presentation and prognosis, Nephrol. Dial. Transplant. 27 (2012) 292–298, 27.
[46] S.M. Sancho-Martínez, L. Prieto-García, M. Prieto, I. Fuentes-Calvo, J.M. López-Novoa, A.I. Morales, C. MartínezSalgado, F.J. López-Hernández, N-acetylcysteine transforms necrosis into apoptosis and affords tailored protection from cisplatin cytotoxicity, Toxicol. Appl. Pharmacol. 349 (2018) 83–93, 349.
[47] J. Luo, T. Tsuji, H. Yasuda, Y. Sun, Y. Fujigaki, A. Hishida, The molecular mechanisms of the attenuation of cisplatin induced acute renal failure by N-acetylcysteine in rats, Nephrol. Dial. Transplant. 23 (2008) 2198–2205.
[48] Z.X. Liu, S.J. Liu, L. Zhou, X.J. Gao, W.Z. Ju, H.S. Tan, C. Yang, Effects of HuangKui capsules on glibenclamide pharmacokinetics in rats, J. Ethnopharmacol. 139 (2012) 1–5.
[49] S. Attaluri, R.R. Bonala, I. Yang, M.A. Lukin, Y. Wen, A.P. Grollman, M. Moriya, C.R. Iden, F. Johnson, DNA adducts of aristolochic acid II: total synthesis and site-specific mutagenesis studies in mammalian cells, Nucleic Acids Res. 38 (2009) 339–352.